A Journal of the Gesellschaft Deutscher Chemiker

Angewandte International Edition GDCh Chemie

www.angewandte.org

Accepted Article

Title: NIR-CPL from chiral complexes of lanthanides and d-metals

Authors: Oliver George Willis, Francesco Zinna, and Lorenzo Di Bari

To be cited as: *Angew. Chem. Int. Ed.* **2023**, e202302358

Link to VoR: https://doi.org/10.1002/anie.202302358

WILEY VCH

10.1002/anie.202302358

WILEY-VCH

MINIREVIEW

NIR-Circularly Polarized Luminescence from Chiral Complexes of Lanthanides and d-Metals

Oliver G. Willis,[a] Francesco Zinna,*[a] and Lorenzo Di Bari*[a]

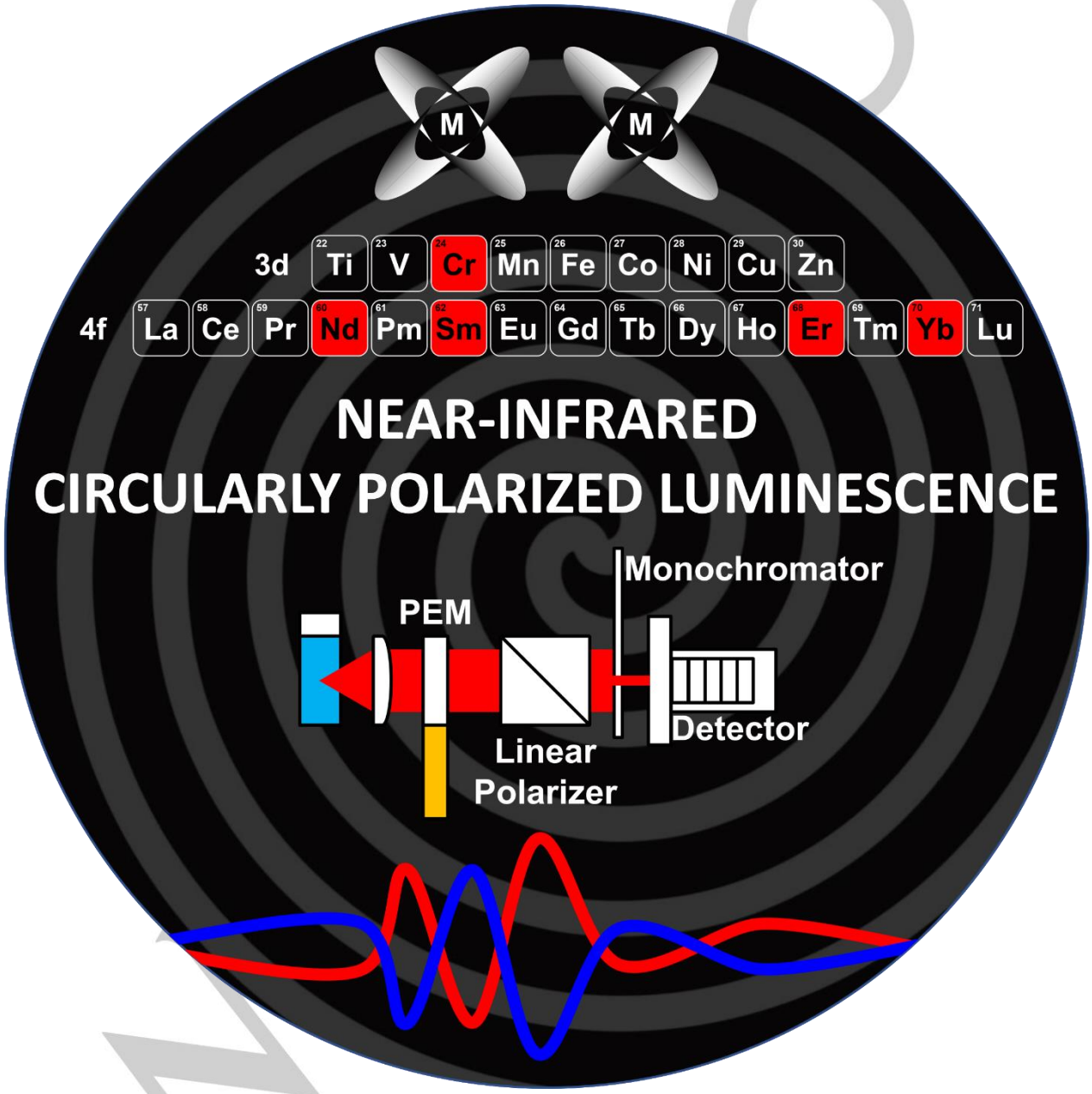

10.1002/anie.202302358

WILEY-VCH

MINIREVIEW

[a] O. G. Willis, Dr. F. Zinna, Prof. L. Di Bari
Department of Chemistry and Industrial Chemistry
University of Pisa
via Moruzzi, 13, 56126, Pisa (Italy)
E-mail: francesco.zinna@unipi.it, lorenzo.dibari@unipi.it

Abstract: In recent years, circularly polarized luminescence (CPL) has witnessed a renaissance, due to the increased popularity of CPL as a spectroscopic technique and greater accessibility to instrumentation. New efficient CPL emitters have been designed and many applications, ranging from electronic devices to microscopy have been proposed. Most examples of CPL are within the visible range, while few cases of near infrared (NIR) CPL active complexes are available. NIR-CPL compounds may have applications in the telecommunication industry, electronic devices and bioassays. In the following, we shall give an overview of the recent developments allowing for the measurements of NIR-CPL, and describe the chiroptical properties of metal complexes which achieve this feat.

1. Introduction

This mini-review aims to provide a comprehensive examination of the recent developments in the measurements of circularly polarized luminescence (CPL) in the near-infrared (NIR) region. CPL has a range of potential applications in fields like security,[1] biology,[2–6] and telecommunications.[7–13]

There has been growing interest in the study of CPL, with a significant number of publications on various emitting species.[1,2,9,10,14–16,16–28] Most of the research has focused on visible light emitters, which may display high quantum efficiencies. However, CPL in the NIR has gained attention as it offers several advantages over visible light for certain applications like bioimaging,[3,16,29–31] and telecommunications.[2,3,9,10,25,29–41] For example, NIR light undergoes low absorption in biological samples, making it easier to obtain high-quality images and preserving the specimen from possible damage. Additionally, low attenuation of NIR light in optical fibers makes it ideal for long-distance communication.

On the other hand, the low intensity of NIR emitters has made it harder to measure CPL in the NIR region. Despite the challenges, improvements in technology and the growing interest in CPL spectroscopy have made NIR-CPL measurement a topic of significant research with promising results.

1.1. The origin of CPL

CPL is quantified by the dissymmetry factor (g_{lum}), representing the degree of preferential emission of left-*vs*-right circularly polarized light. This value is the ratio of the transition rotational strength (R_{ij}) to the transition oscillator strength (D_{ij}), as expressed in the following equation (in cgs units):[42]

$$g_{lum} = 4\frac{R_{ij}}{D_{ij}} = 4\frac{\left|\vec{\mu_{ij}}\right|\left|\vec{m_{ij}}\right|}{\left|\vec{\mu_{ij}}\right|^2 + \left|\vec{m_{ij}}\right|^2}\cos\theta \quad (1)$$

The initial and final states are represented as i and j; μ_{ij} represents the electric transition dipole moment (ED), m_{ij} represents the magnetic transition dipole moment (MD); and θ is the angle between the electric and magnetic transition dipole moments. The g_{lum} can be expressed experimentally as Eq 2, where I_L and I_R, correspond to the intensity of left and right circularly polarized light, respectively.

$$g_{lum} = \frac{\Delta I}{I} = \frac{I_L - I_R}{\frac{1}{2}(I_L + I_R)} \quad (2)$$

Eq. 1 shows that the $|g_{lum}| = 2$ if θ = 0 (or 180°) and $\left|\vec{\mu_{ij}}\right| = \left|\vec{m_{ij}}\right|$. This reveals that the common thought that simply maximizing the magnetic contribution while minimizing the electronic, overall increases the dissymmetry ratio is a misconception.

1.2. B_{CPL} in the context of complex lanthanide and d-metal CPL emission

In 2021,[43] the concept of circular polarization brightness (B_{CPL}) was introduced. Beside g_{lum}, B_{CPL} factors in the extinction coefficient (ε_λ) and quantum yield (ϕ). For lanthanides and d-metal complexes which typically show signals of opposite overlapping transitions, the analysis is made difficult. Thus, the branching ratio (β_i) was added to assess the brightness for individual transitions. Eq 3 shows the formula for B_{CPL} where I_i is the integrated intensity of the considered transition and $\sum_j I_j$ is the summation of the integrated intensities over all the transitions.

$$B_{CPL} = \frac{I_i}{\sum_j I_j} \times \varepsilon_\lambda \times \phi \times \frac{|g_{lum}|}{2} = \beta_i \times \varepsilon_\lambda \times \phi \times \frac{|g_{lum}|}{2} \quad (3)$$

In case of CPL spectra with several opposite bands within the same manifold, a more general definition of B_{CPL} factor has to be applied:

$$B_{CPL} = \varepsilon_\lambda \times \phi \times \frac{1}{2}\frac{\int_a^b g(\lambda) \times I(\lambda)\, d\lambda}{\int_i^j I(\lambda)\, d\lambda} \quad (4)$$

Where the integral in the numerator runs within the limits of the considered transition, while the integral in the denominator covers the whole emission range. In general, B_{CPL} quantifies the overall signal available for the CPL measurements. Therefore, provided detector sensitivity and set-up efficiency are equal, compounds with a similar B_{CPL} are expected to show a similar CPL signal-to-noise ratio.

1.3. CPL of lanthanide and d-metal complexes

If we consider Ln-centered f-f transitions as purely intraconfigurational, then they are ED forbidden and MD allowed. We can rationalize that the necessary ED to provide non

10.1002/anie.202302358

vanishing rotational strength can be accounted for by two limiting mechanisms: static and dynamic coupling.

Static coupling is responsible for the 4f and 5d orbitals mixing in an asymmetric environment. It provides odd parity interconfigurational character ($\mu_{ij} \neq 0$) due to the covalent interaction between the ligand and metal center. This can only occur when the first coordination sphere is chiral. The chiroptical properties of complexes with an achiral first coordination sphere can only be explained by the dynamic coupling scheme.

One must recall that MD transitions of the lanthanide can be associated with an electric quadrupole transition moment (EQ). In turn, this can dynamically couple with ED moments of polarizable linear oscillators in the nearby chromophore carried by the ligand. This dynamic coupling has the effect of providing an ED to the lanthanide-centered MD transition and non-vanishing rotational strength follows.[44] This may result in transitions with strong chiroptical properties compared to simple static coupling.

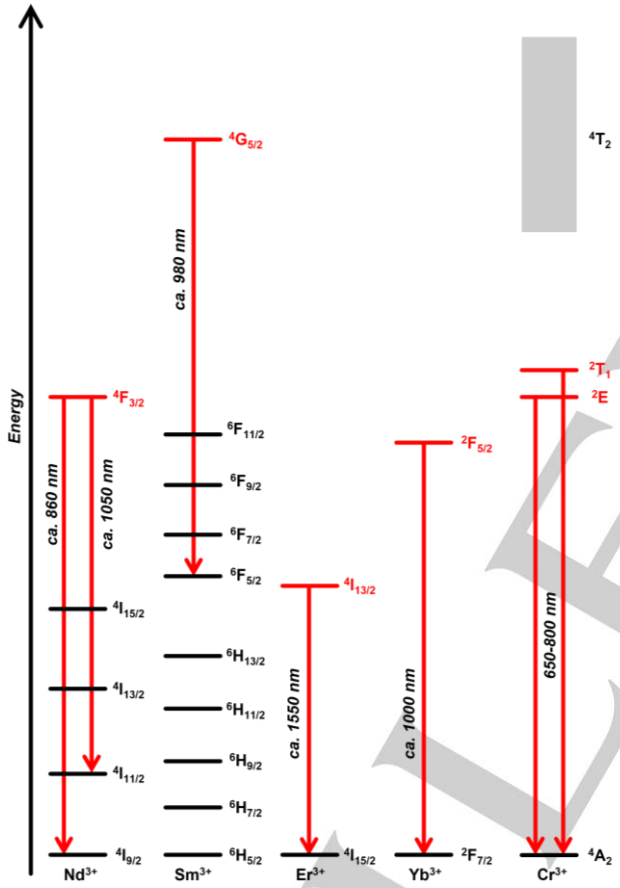

Figure 1. Dieke diagram of the energy levels of NIR emissive trivalent lanthanide ions and the energy levels of Cr^{3+}.

In 1980, Richardson developed selection rules which govern the magnitude of chiroptical properties in optically active lanthanide(III) complexes that result from 4f-4f transitions.[45] These rules are established by considering the effects of spin-orbit coupling and crystal field interactions on the S, L, and J quantum numbers. The transitions between different terms of lanthanides are classified based on their estimated electric dipole strength (EI > EII > EIII > EIV), rotational strength (RI > RII > RIII > RIV), and dissymmetry factor (DI > DII > DIII) in a chiral environment.[45]

The d-metals display transitions stemming mostly from charge transfer, which seldom results in strong CPL activity. Octahedral Cr(III) complexes are an exception because of their large crystal field stabilization energy, caused by their d^3 electronic configuration and their strongly ED-forbidden, MD-allowed transitions. Octahedral Cr(III) complexes with strong ligand fields are known to exhibit magnetically allowed spin-flip (SF) emissions in the 650-800 nm range, such as the Cr($^2E \rightarrow {}^4A_2$) and Cr($^2T_1 \rightarrow {}^4A_2$) transitions (Figure 1).[46–54] Despite being electric-dipole forbidden, carefully engineered ligands can shift the metal-center $^4T_2$ state higher in energy, thus preventing back-intersystem crossing, which would deactivate the emissive SF state.[55,56] These factors make Cr(III) ideal NIR-CPL emitters, opposed to other metals (Ru, Ir, Pt or Au).[57]

1.4. The basic components of CPL instrumentation and its extension to the NIR

In a CPL spectrofluoropolarimeter, a light source, such as a laser diode, LED, or lamp is used to excite the sample. Polarization optics typically include a photoelastic modulator (PEM) and a linear polarizer with axes reciprocally oriented at ±45 degrees. This is followed by a monochromator, and finally a detector. Detectors for CPL and CD spectroscopy are typically photomultiplier tubes (PMT) or solid-state avalanche photodiodes (APD), which work to intensify weak signals. Most standard photocathodes in PMTs and CCDs are only sensitive in the visible window, so to measure weak NIR emission, specialized detectors such as liquid nitrogen-cooled InGaAs detectors are used.[9,10] Alternatively, when dealing with large *g*-values, the PEM can be replaced by a less expensive quarter-waveplate (QWP). Recently, based on this principle, new examples of CPL instrumentation were reported. For example, the two CP components, formed after passing through a QWP, can be directed into two orthogonal directions by a LP beam splitter. The signal is then detected either by two balanced CCD detectors[58] or by a single one, where the two oppositely polarized beams are spatially separated onto the grating of the CCD camera.[59] This set-up allows the CPL measurements of compounds with a $B_{CPL} \geq 0.5\ M^{-1}\ cm^{-1}$, a performance comparable with PEM-based set-ups.[59]

2. NIR-CPL of lanthanide complexes

10.1002/anie.202302358

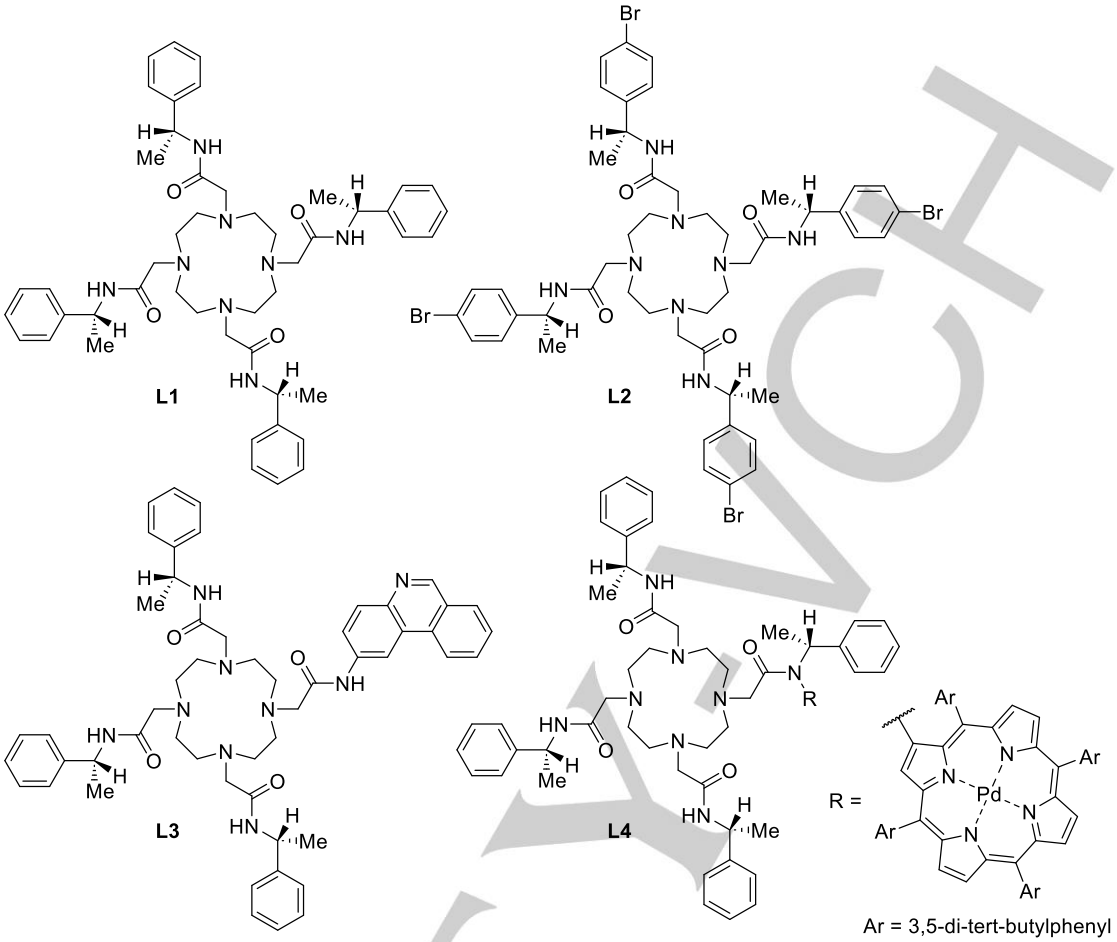

Scheme 1. Cyclen-based ligands designed by Parker and co-workers.[29–31]

10.1002/anie.202302358

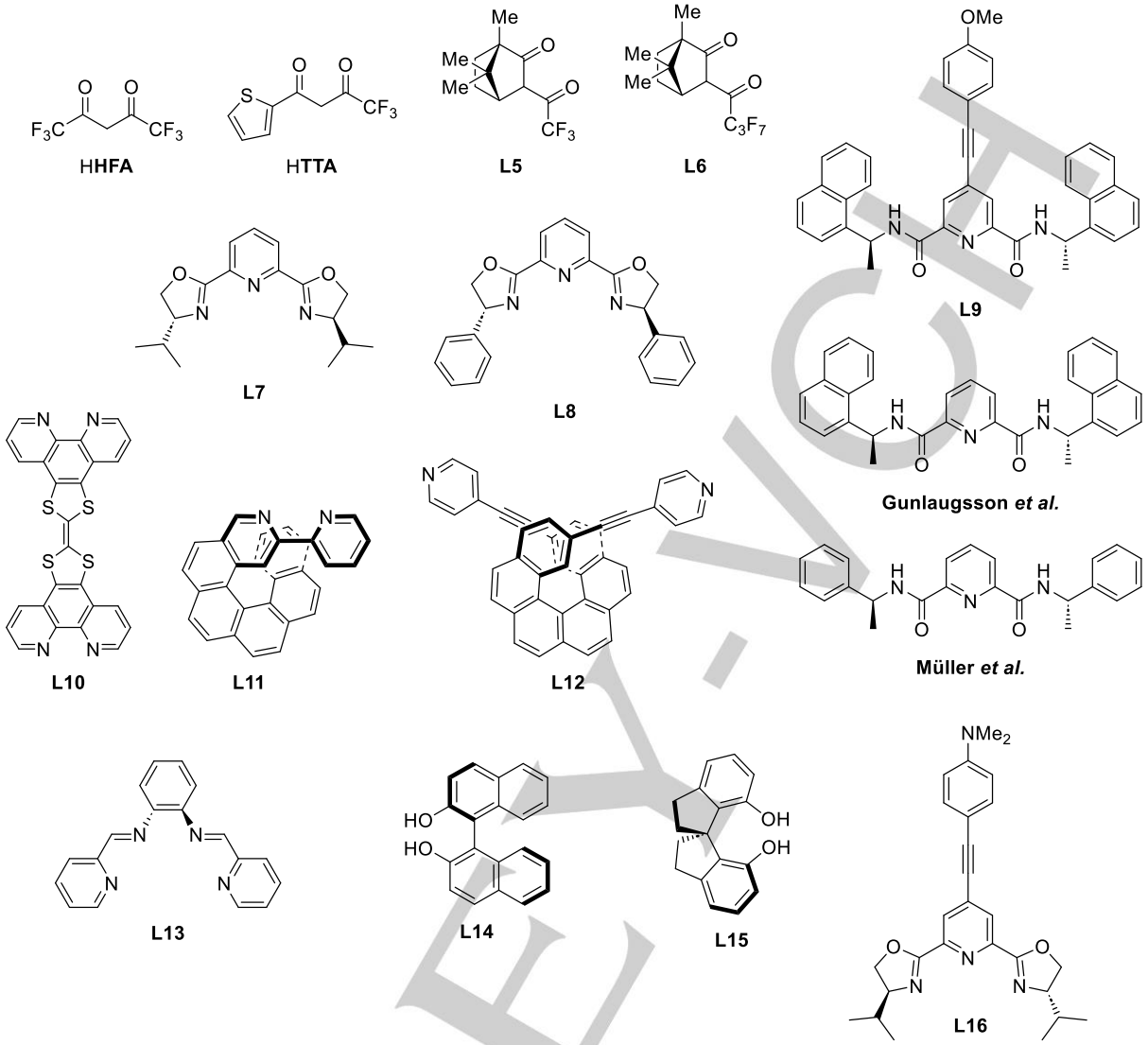

Scheme 2. Structures of the ligands employed in NIR-emissive chiral lanthanide complexes.

The first report of NIR-CPL was published by Parker *et al*., in 1998, where they complexed Yb with a cyclen-based ligand (**L1**, Scheme 1).[31] The complexes were formed from a 1,4,7,10-tetraazacyclododecane chelate, which is known for binding strongly to lanthanide ions and forming C_4 structures with chirality derived from the phenylethylamine moieties.[60,61] Yb has one intraconfigurational term-to-term transition ($^2F_{5/2} \rightarrow {}^2F_{7/2}$, Figure 1). Richardson's selection rules predict this transition to show a relatively strong dipole strength (EI), rotational strength (RI), and moderate/high dissymmetry values (DII).[45] The complex exhibited reasonable emission properties and a measurable degree of CPL.

Follow-up publications in 1999 and 2000 expanded on this seminal work, detailing the NIR-CPL of several other Yb complexes coordinated with modified 1,4,7,10-tetraazacyclododecane chelates (**L2-4**, Scheme 1).[29,30] The authors noted that despite slight structural changes, the CPL spectra retained a similar sign, shape and intensity for all complexes, indicating a consistent C_4 structure with almost regular square antiprismatic coordination. Dissymmetry values of around 0.2 were reported for all cyclen-based Yb complexes measured.[29–31] The complex Yb(**L5**)$_3$ (**L5** = (−)-3-(trifluoroacetyl)camphor = facam, Scheme 2) in dimethyl sulfoxide was chosen as a standard, due to its commercial availability, and because the Eu analogue is routinely used as a reference for CPL measurements in the visible.[42] The Yb(**L5**)$_3$ complex showed a measured $|g_{lum}|$ value of 0.076 at 975 nm corresponding to the peak maxima.

Along with the Yb complexes, Parker *et al*., also complexed Nd with **L4** (Scheme 2). Nd has two transitions occurring in the NIR (Figure 1): (i) $^4F_{3/2} \rightarrow {}^4I_{9/2}$ (ca. 860 nm) and (ii) $^4F_{3/2}$ to $^4I_{11/2}$ (ca. 1050 nm). Both transitions do not satisfy magnetic dipole selection rules which results in weaker chiroptical activity compared to the Yb transition. Indeed, the measured CPL spectrum shows g_{lum} values of around 10^{-3}, much lower in comparison to other lanthanide transitions.[29]

To achieve these pioneering measurements of NIR-CPL, existing components of a commercial Spex Fluorolog II spectrofluorometer, including a Xe arc-lamp excitation source and monochromators were utilized. A 50 kHz PEM was followed by a linear polarizer. The emission was detected using a liquid N_2-cooled photomultiplier tube (PMT). A schematic diagram of the first NIR-CPL setup is shown in figure 2.[29]

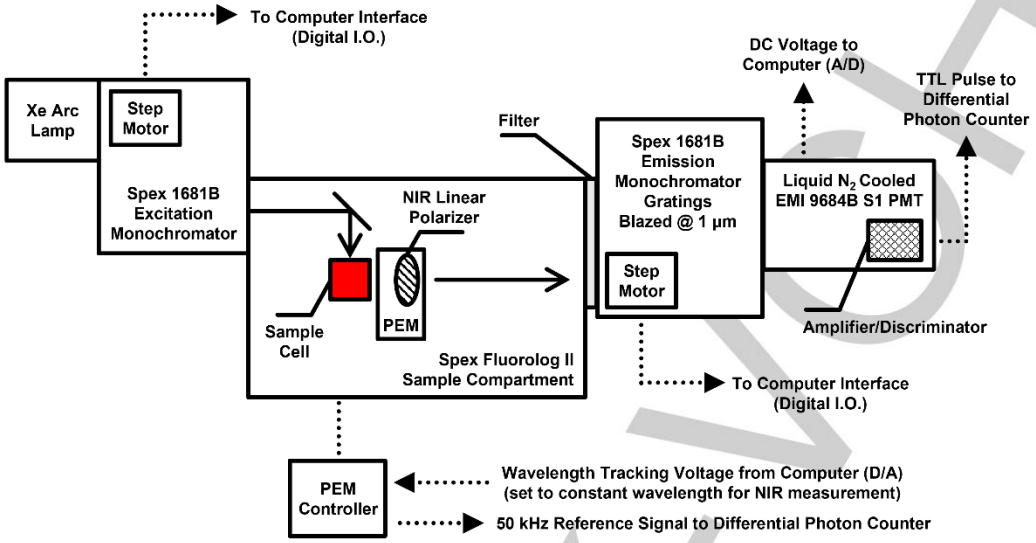

Figure 2. Schematic diagram for instrumentation used to measure NIR-CPL by Parker and co-workers (adapted with permission from Ref 29. Copyright 2000 American Chemical Society).

It was not until two decades after Parker's pioneering work that Di Bari's group published their own measurements of NIR-CPL in 2019.[3] Despite the growing popularity of CPL as a spectroscopic technique, such a gap highlights the limitation in terms of equipment and molecular compounds suitable for NIR-CPL measurements.

To address the limited number of suitable NIR-emissive chiral lanthanide complexes, Di Bari's group designed heteroleptic complexes that offered good modularity and tunability. This allowed them to optimize both total luminescence and circular polarization independently. The ligand, 4,4,4-trifluoro-1-(thiophen-2-yl)butane-1,3-dione (H**TTA**, Scheme 2) was used to act as the lanthanide antenna, as $Yb(TTA)_3$ is known to show reasonable quantum yields.[62,63] The coordination sphere was easily completed by adding commercially available enantiopure chiral pyridine bis(oxazoline) (PyBox) derivatives shown as **L7** and **L8** in Scheme 2. These chiral ligands aimed to induce the structural rearrangement of the sensitizing ligands to form a stereo-ordered system.

To measure CPL in the NIR, Zinna *et al.* modified their existing CPL spectrometer, previously used for visible emissive species.[64] The CPL setup utilized a PEM coupled with an uncoated Glan-Thompson polarizer. A PMT with an Ag-O-Cs photocathode was used to detect the weak NIR signals (Figure 3).[3]

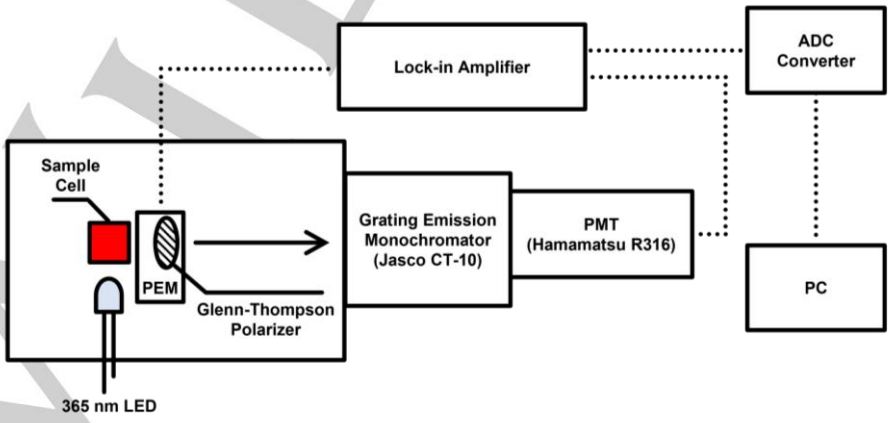

Figure 3. Schematic diagram for instrumentation used to measure NIR-CPL by Zinna and Di Bari.

10.1002/anie.202302358

The complexes gave quantum yields of around 0.7% similar to other NIR-emitting molecular complexes, while the CPL showed intense bands with varying signatures for each complex (Figure 4). Both complexes showed $|g_{lum}|$ values of 10^{-2} and B_{CPL} values of ca. 4 M^{-1} cm^{-1}, reasonable for NIR-CPL active complexes, considering the expected low quantum yields (< 1%).[3,43]

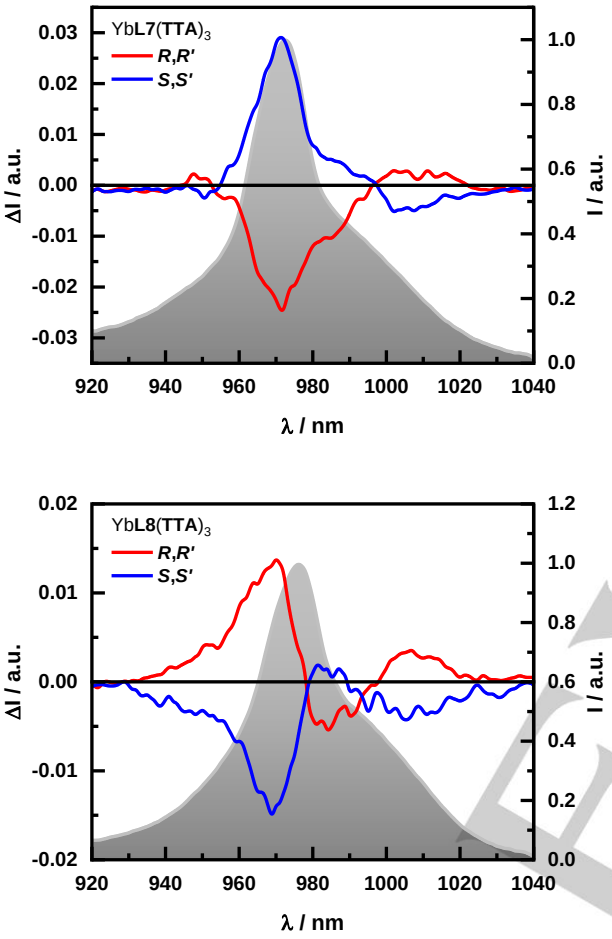

Figure 4. Top: NIR-CPL spectra of Yb**L7**(**TTA**)$_3$ (top) and of Yb**L8**(**TTA**)$_3$ (bottom). Normalized average total emission is traced in the background. All complexes were measured in 6 mM CH_2Cl_2 solutions under 365 nm irradiation at room temperature (reproduced from Ref. 3 with permission of The Royal Chemical Society).

The most intense transition arises from the fundamental 1 ← 1' (where 1 is the lowest level of the ground state and 1' is the lowest level in the excited state), while the lower energy transitions were assigned to 2, 3, 4 ← 1' . Due to weak interaction of the crystal field, the various Stark levels of the ground and excited state likely have significant Boltzmann population, meaning many transitions are likely occurring simultaneously (e.g., from hot bands), leading to a more complex assignment. Sophisticated computational studies and low temperature measurements would be required for more in-depth assignments.[32,34,35,65–69]

When evaluating the NIR-CPL spectrum of Yb, it is important to discuss the balance of positive and negative signals over the entire transition. Due to Yb possessing only one intraconfigurational transition, if it can be considered decoupled from the environment (pure static coupling), one expects the integral over the entire CPL spectrum around 1000 nm to be zero.[23] The observed imbalance of one sign over the other is a strong suggestion of dynamic coupling between the lanthanide transition and the polarizable diketonate ligands.

Maury and co-workers[35] synthesized homoleptic complexes from ligands adapted from groups led by Gunlaugsson[70] and Müller[71]. The complex, constructed from a ligand (**L9**, Scheme 2) featuring an extended chromophore unit, in position 4 to pyridine core, was thoroughly investigated through chiroptical studies and *ab initio* crystal-field characterizations to fully assign the NIR-CPL spectrum. The electronic structure of the chiral Yb complex was characterized through a combination of techniques including absorption and luminescence carried out in ambient conditions and low temperature, as well as in solution and solid state.

Taking advantage of variable temperature measurements and with a theoretical support, the energy of all electronic substates of the ground ($^2F_{7/2}$) and excited ($^2F_{5/2}$) manifold were determined and the individual rotational strengths calculated. This showed that the measured spectrum is a superposition between all possible transitions.

The NIR-CPL of the complex was also measured using two different setups. Firstly, a conventional PEM with a single channel detector was used, and secondly, a CCD camera and static optics were used which provide better resolution but are limited by the sensitivity of the Si sensors.

The same in-depth analysis was performed on Yb**L11**(**HFA**)$_3$ and a polymeric [Yb**L12**(**HFA**)$_3$]$_n$ system, both featuring intrinsically chiral helicene derivatives.[32] The mononuclear complex displays a g_{lum} that is over 16 times higher than the corresponding enantiopure polynuclear system, while also showing an inverted signal between each absolute isomer at 978 nm corresponding to the most intense transition. The decrease in CPL intensity of the polynuclear system is likely a result of the increased separation between the chiral helicene ligand and the lanthanide core. In fact, the NIR-CPL of the polymeric system appears to be at the edge of the detection limit, with *g*-values on the order of 10^{-3}. The simulated spectrum shows contributions from all possible transitions, which again makes the assignment of the observed CPL spectra difficult. Calculated rotational strengths of Yb**L11**(**HFA**)$_3$ are 1.3 times higher than those of [Yb**L12**(**HFA**)$_3$]$_n$, in line with experimental observations. On the other hand, the calculations could not predict the change in sign observed for the zero-line transition.

A dinuclear Yb complex that showed strong NIR-CPL was reported in 2021.[34] It was constructed based on the principles demonstrated earlier for heteroleptic complexes, which have separate sensitizing and chiral-inducing ligands.[3] For the dinuclear complex, two chiral Yb(**L5**)$_3$ units were bridged with a bis(1,10-phenantro[5,6b])tetrathiafulvalene triad (**L10**), which acts as the light harvesting portion of the dinuclear complex. Despite no change in the position of the CPL bands, a significant decrease in intensity was observed in the solid state. In addition to the signal drop-off, the shape and sign were completely altered, with a sign reversal for the most intense transition. In solution, [Yb**L10**(**L5**)$_3$]$_2$ showed a g_{lum} of 0.013 at 977 nm, while for the same absolute configuration in the solid state, a g_{lum} of −0.001 was found. The authors attributed these significant changes to the modification of the environment surrounding the lanthanide core, as well as a reduction of the population of conformers in the solid state.

10.1002/anie.202302358

Piccinelli *et al.* in 2022 reported the first NIR-CPL measurements in aqueous, non-deuterated media.[33] This result was achieved by embedding the chiral [Yb**L13**$(TTA)_2]^+$ complex in poly lactic-co-glycolic acid (PLGA) nanoparticles. With this strategy, quenching of the excited state through multi-phonon processes was limited, allowing the measurement of a relatively strong CPL. Moreover, the PLGA nanoparticle enables water solubility and increases stability of the [Yb**L13**$(TTA)_2]^+$ complex in water. These measurements are particularly intriguing in view of potential applications such as NIR-CPL bio-assays or trackers for CPL microscopy.

A study by Ung in 2022 reported the first measurement of NIR-CPL of samarium between 925 and 1025 nm (Figure 1).[25] The Sm complex $[Na(THF)_2]_3Sm($**L15**$)_3$ (Scheme 3) was coordinated with 1,1'-spirobiindane-7,7'-diol (**L15**), which, thanks to the intrinsically chiral nature and rigid spiro sp^3 carbon, improves both the quantum efficiency (2.8%) and CPL ($|g_{lum}|$ = 0.17 at 980 nm) of the Sm NIR emission (B_{CPL} = 6.9 M^{-1} cm^{-1}).[25] The Sm complex was inspired by the rare earth metal bimetallic (REMB) complex $[Na(THF)_2]_3Ln($**L14**$)_3$ (Scheme 3) first reported by Shibasaki in 1992,[72] which contains axially chiral 1,1'-bi-2-naphthol antennae ligands. The NIR-CPL spectrum of $[Na(THF)_2]_3Sm($**L15**$)_3$ shows two main transitions occurring at 980 nm which can be attributed to the $^4G_{5/2} \rightarrow {}^6F_{5/2}$ transition, while the less intense band at 940 nm is likely a combination of the $^4G_{5/2} \rightarrow {}^6F_J$ (J =1/2, 3/2) and $^4G_{5/2} \rightarrow {}^6H_{13/2}$ transitions (Figure 1).[25] The strength of the CPL signal obtained is likely due to the contribution of the $^4G_{5/2} \rightarrow {}^6F_{3/2}$ transition, which belongs to class RII (Figure 1).[45]

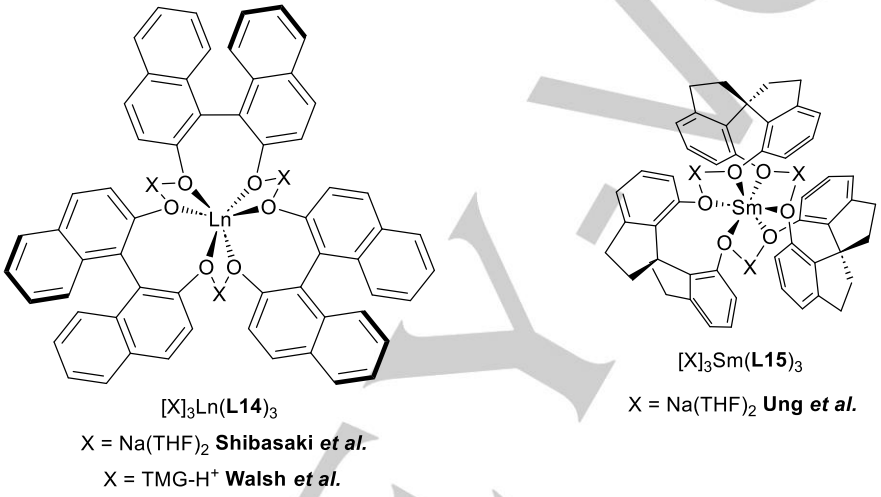

$[X]_3Ln($**L14**$)_3$
X = $Na(THF)_2$ **Shibasaki *et al.***
X = TMG-H^+ **Walsh *et al.***

$[X]_3Sm($**L15**$)_3$
X = $Na(THF)_2$ **Ung *et al.***

Scheme 3. The pin-wheel structures of the REMB type complexes developed by Shibasaki,[72] Walsh,[73] and Ung.[25]

The group of Di Bari and Zinna carried out a study to expand the understanding of NIR chiroptical properties of lanthanide complexes.[2] Two sets of homoleptic complexes of Yb, Tm and Er were prepared. The first was based on CsLn(**L6**)$_4$, while the second was a water and air-stable analogue of Shibasaki's original complex designed by Walsh and co-workers.[73] Beside Yb transition, Er $^4I_{13/2} \leftrightarrow {}^4I_{15/2}$ (~1500 nm) are predicted to show strong chiroptical activity (Figure 1). Two cases of strong NIR-CPL from the Yb complexes were reported, with $|g_{lum}|$ values of 0.38 for CsYb(**L6**)$_4$ at 988 nm and a maximum of 0.07 at 954 nm for $[TMG{-}H^+]_3$Yb(**L14**)$_3$. The NIR-CPL of CsYb(**L6**)$_4$ also shows a monosignate band (Figure 5), which is a result of strong dynamic coupling.

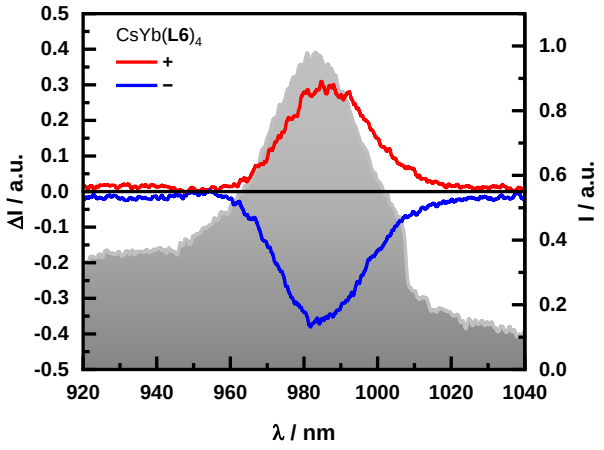

Figure 5. NIR-CPL spectra of the CsYb(**L6**)$_4$ enantiomers with normalized average total emission traced in the background. Complexes were measured in 1 mM CH_2Cl_2 solutions under 365 nm irradiation at room temperature (reproduced from Ref. 2 with permission of The Royal Chemical Society).

10.1002/anie.202302358

The $|g_{lum}|$ observed for CsYb(**L6**)$_4$ is the highest recorded value to date for any Yb complex. By studying the NIR circular dichroism (CD) of CsEr(**L6**)$_4$ and [TMG−H$^+$]$_3$Er(**L14**)$_3$, the work concluded that the $^4I_{13/2} \rightarrow {}^4I_{15/2}$ transition of Er falling in the 1400–1600 nm region could also show strong CPL (Figure 1).[2]

The range of NIR-CPL detection was extended further by the groups of Ung and Di Bari, who working independently and simultaneously both published NIR-CPL of Er at ca. 1550 nm.[9,10] This wavelength domain is interesting for free-space long-distance communication such as in fiber optics and light detection and ranging (LIDAR) with the emission profile located within the telecommunication C-band.[7,8,74]

Progressing further into the NIR, increases the detrimental effect of quenching by multi-phonon processes which lowers the overall quantum efficiency of the system, making even strong CPL activity difficult to measure. For measurements within this region, it is also important to have appropriate optics and sensitive detectors.

To measure the strong NIR-CPL of Er, two aspects needed addressing: (i) Design of chiral Er complexes which show both intense emission and strong CPL. (ii) A new experimental setup, beyond those commercially available. Ung addressed the first issue by studying the REMB Shibasaki's, [Na(THF)$_2$]$_3$Er(**L14**)$_3$ complex.[10] The structure is antiprismatic, however the binaphtholate chromophores are able to transfer energy to the acceptor states of the Er(III) ion and to provide significant dynamic coupling. Indeed, remarkable strong NIR-CPL was measured for this complex. The complex showed high quantum efficiencies of 0.58% and a maximum $|g_{lum}|$ of 0.47 at 1540 nm corresponding to a B_{CPL} of 57.3 M^{-1} cm^{-1}.[10] This work also reported a second example of NIR-CPL of Nd between 840 and 1150 nm with maximal $|g_{lum}|$ values of 0.04 and 0.03 at 900 and 1040 nm respectively.[10]

The group of Di Bari approached the challenge differently. To this end, a purposely tuned novel ligand (**L16**) featuring the strong chiral inducer PyBox core, with an extended chromophore unit were synthesized.[9] This complex [Er(**L16**)$_2$]$^{3+}$, displayed strong CPL activity (Figure 6), with a maximum $|g_{lum}|$ of 0.33 at 1539 nm (B_{CPL} = 0.7 M^{-1} cm^{-1}).[9] Through lifetime measurements, the sensitization efficiency was calculated, giving a value of 75%. This high value indicated (i) the suitability of the ligand design to sensitize Er; (ii) that the predominant loss of energy is through quenching of the populated excited lanthanide state.

Concerning instrumentation, both groups used similar methodologies involving manual rotation of a static QWP. The group led by Ung used an OLIS NIRCPL Solo, which was pre-equipped with a static QWP.[10] Di Bari and Zinna custom designed and 3D-printed dedicated holders for both QWP and linear polarizer, such that they could be placed within the sample compartment of a Horiba Jobin-Yvon Fluorolog®-3 spectrofluorometer.[9] In both cases, cooled InGaAs detectors were used.

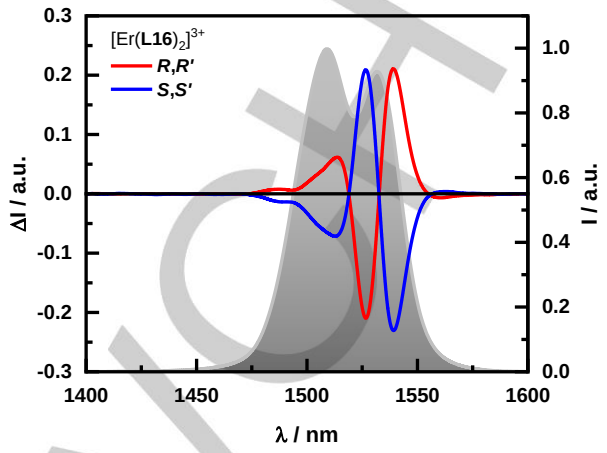

Figure 6. NIR-CPL spectra of the [Er(**L16**)$_2$]$^{3+}$ enantiomers with normalized average total emission traced in the background. Complexes were measured in 0.01 mM $CDCl_3$ solutions under 450 nm irradiation at room temperature (reproduced from Ref. 9 with permission from Wiley).

Interestingly, NIR-CD of the same Er $^4I_{13/2} \leftrightarrow {}^4I_{15/2}$ shows practically superimposable features to those observed in CPL. Recently, Di Bari *et al* published a second article on Er NIR-CPL from various "untuned" hetero and homoleptic complexes.[75] In general, the same empirical rules and stereochemical principles, used to design visible Ln emitters with high g_{lum} factors, apply to NIR Ln emitters. A further caveat in the case of particularly low energy emitters, such as Er, may be in order. The complexity of its ground and excited electronic structure in terms of M_J levels, with all states virtually populated at room temperature, may lead to up to 56 transitions (assuming a non-cubic environment and Starck sub-levels being doubly degenerate) in the CPL spectrum within ~100 nm.[2,76] Such transitions can possess opposite signs which can overlap and cancel in spectra recorded with standard wavelength resolution. In the worst case, this can lead to an observed vanishing CPL. In higher symmetries, the number of non-degenerate transitions is greatly reduced, which possibly alleviates the issue.

3. NIR-CPL of d-metal complexes

10.1002/anie.202302358

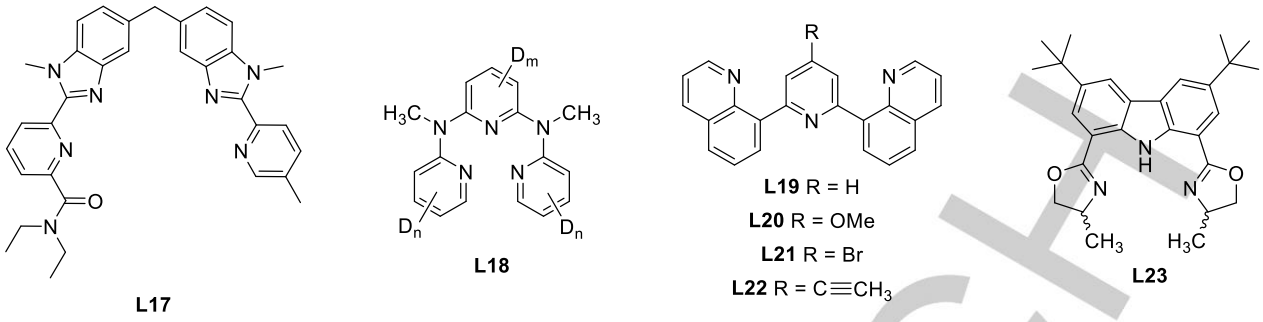

Scheme 4. Structures of the ligands employed in NIR-emissive chiral Cr(III) complexes.

The first example of CPL for a chiral Cr(III) complex was reported in the early days of CPL, in 1967 by Emeis and Oosterhoff.[77] The $Cr(en)_3(ClO_4)_3$ (en = ethylenediamine) complex was showed a g_{lum} of 0.028 at 610 nm.[77] Interestingly, this was one of the first ever examples of CPL. The first report of CPL in the NIR of a chiral Cr(III) complex was in 2003 by Piguet and co-workers from the complex, $[EuCr(\mathbf{L17})_3]^{3+}$.[41] $[Cr(\mathbf{L17})_3]^{3+}$ has a unique triple-helical receptor structure, which allows for the preparation of enantiomerically pure nonadentate podands. The chirality of the complex is derived solely from the helical structure. Upon recombination with Eu(III), inert and enantiomerically pure triple-stranded lanthanide helicates are formed. The bimetallic $[EuCr(\mathbf{L17})_3]^{3+}$ complex displays an emission band centered at 745 nm originating from the $^2E \rightarrow {}^4A_2$ (Figure 1) transition with an associated $|g_{lum}|$ of 0.01 which is similar to the earliest reports of NIR-CPL from Yb complexes.[41]

For the purpose of this report, and the limited number of Cr(III) complexes which emit classical NIR emission (780 to 2500 nm), all systems which show maxima around 750 nm and tail off past 780 nm will be discussed.

Despite this interesting and rare report of NIR-CPL from an earth-abundant chiral emitter, there was no report for the next 15 years similar to the case of NIR-CPL of lanthanide complexes.

This changed, however, in 2019 when both Piguet[39] and Seitz[40] published separate works on the NIR-CPL of Cr(III) compounds. Piguet *et al*. published their measurements of the chiral SF luminophore $[Cr(\mathbf{L19})_2]^{3+}$. The two enantiomers were easily separated from the racemate *via* chiral HPLC and upon excitation at 355 nm, two distinct, sharp emission bands at 747 nm and 724 nm, corresponding to the SF $Cr(^2E \rightarrow {}^4A_2)$ and $Cr(^2T_1 \rightarrow {}^4A_2)$ transitions were observed (Figure 1). The CPL spectra showed a corresponding bisignate signal. Dissymmetry values of 0.2 and 0.1 for the $Cr(^2E \rightarrow {}^4A_2)$ and $Cr(^2T_1 \rightarrow {}^4A_2)$ transitions were measured, which are comparable to the MD-allowed, ED-forbidden f-f transitions.[39]

Seitz *et al*. developed a molecular ruby complex, $[Cr(\mathbf{L18})_2]^{3+}$ which showed high phosphorescence quantum yields of up to 30%.[40] Despite the difficulty in the separation, the enantiomers proved to be kinetically inert. The $[Cr(\mathbf{L18})_2]^{3+}$ is pseudo-octahedral with a local D_2 symmetry making the complex chiral. A broad emission profile from 700 to 840 nm is observed corresponding to the NIR luminescence band $^2E/^2T_1 \rightarrow {}^4A_2$ (Figure 1). The maximum of the emission was at 775 nm and showed a $|g_{lum}|$ value of 0.093, and a remarkable B_{CPL} of 418.5 $M^{-1}cm^{-1}$.

Piguet explored the NIR-CPL of Cr(III) complexes further by synthesizing derivatives of the original ligand (**L19**) by functionalizing para to the pyridine (**L20**-**22**, Scheme 4), effectively tuning the electronic properties of the complex. The modification of ligand **L19** through addition of the bromo (**L20**), methoxy (**L21**) and alkyne unit (**L22**) had little impact on the structural features of the complex, meaning that for each derivative, the sign, shape, and intensity of the CPL spectra were identical to the parent complex $[Cr(\mathbf{L19})_2]^{3+}$.[38] Thanks to the efficient quantum yields (ca. 15 %) and high $|g_{lum}|$ values (ca. 10^{-1}), high B_{CPL} values ranging from 76.5 M^{-1} cm^{-1} for $[Cr(\mathbf{L20})_2]^{3+}$ to 173 for $[Cr(\mathbf{L22})_2]^{3+}$ were obtained.[38]

The two limitations of the previously discussed chiral Cr(III) complexes can be conveniently categorized and explained by two published works in 2023. Firstly, the need for chiral separation, being **L17**-**22** ligands not intrinsically chiral, limits the tuneability and possible future large-scale preparations. Secondly, all reports mentioned previously are recorded in de-aerated and/or deuterated conditions which substantially limits the complex use in many potential applications.

The first issue is addressed by Lu and Yang,[37] in which the helical chirality of the Cr(III) complex is controlled by the presence of a stereogenic carbon in **L23**. The complex $[Cr(\mathbf{L23})_2]^+$ shows a single broad emission profile with a $|g_{lum}|$ value of ca. 0.002 in both solution and solid-state at 845 nm.[37] The low dissymmetry value compared to the other reports is attributed to mixing of electronically dipole-allowed charge-transfer transitions in the excited states.

The second issue was tackled by encapsulating the previously measured $[Cr(\mathbf{L19})_2]^{3+}$ complex in silica nanoparticles.[36] The silica matrix has very little interaction with the Cr(III) complex as seen by the consistent g_{lum} for both encapsulated and naked complexes. The silica matrix acts to prevent triplet oxygen quenching and limiting vibrational motion and subsequent deactivation pathways. These effects are congruent with increased quantum efficiencies and lifetimes, larger than that of the non-encapsulated complex under aerobic conditions by a few orders of magnitude.

10.1002/anie.202302358

4. Conclusions and perspectives

Thanks to the rational design of suitable ligands and technological advancements which is making CPL measurements more accessible, an increasingly growing number of reports of CPL in the NIR originating from complexes of lanthanides and d-metals have been published. Although the field is still at the beginning, the rare reports of NIR-CPL show remarkably high dissymmetry values and good B_{CPL}, sometimes higher or comparable with common purely organic visible emitters. The strong CPL character of ED-forbidden, MD-allowed transitions are extremely important for the implementation of chiral emissive systems in many potential applications, ranging from bioimaging (joining the specificity of CPL reported with the advantage of NIR emission) to the telecommunications industry, including chiral electronic devices. To this end, besides solution, solid state measurements of NIR-CPL will need to be carried out, overcoming possible experimental set-up limitations, in terms of sensitivity and artifacts. With further progress in experimental and theoretical data, one can envisage that even better performing systems will be designed and synthesized, with new possibilities in the field being opened up.

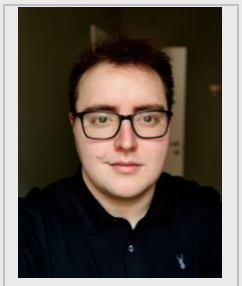

Oliver G. Willis graduated as a Master of Chemistry from Durham University in 2020. Then, he took up a PhD position at the Univeristy of Pisa under the supervision of Prof. Lorenzo Di Bari, working as part of the Marie Curie HEL4CHIROLED ITN with the main research goal to develop chiral lanthanide complexes which emit strong CPL for applications in CP-OLEDs.

Francesco Zinna earned his PhD in 2016 at the University of Pisa. He then worked as a postdoctoral assistant at the University of Geneva with Prof. Lacour. Since 2018, he is an assistant professor in the Chemistry and Industrial Chemistry Department at the University of Pisa. In 2022 he was awarded the Ciamician Medal of the Italian Chemical Society for his contributions to the development of frontier chiroptical techniques.

Lorenzo Di Bari is a Professor of Organic Chemistry at the University of Pisa, where from 2018 to 2022 he was the head of the Department of Chemistry and Industrial Chemistry. His research focuses on the development of experimental methods for the stereochemistry of organic and inorganic compounds and on scouting new applications of chiroptical properties.

Acknowledgements

O.G.W thanks financial support of the European Commission Research Executive Agency, Horizon 2020 Research, and Innovation Programme under the Marie Sklodowska-Curie grant agreement No. 859752-HEL4CHIROLED-H2020-MSCAITN-2019. The Italian Ministero dell'Università, PRIN 20172M3K5N is acknowledged for fundings.

Keywords: Infrared • CPL • Circularly Polarized Luminescence • CPL Instrumentation • Chiroptical properties

[1] L. E. MacKenzie, R. Pal, *Nat. Rev. Chem.* **2021**, *5*, 109–124.
[2] O. G. Willis, F. Zinna, G. Pescitelli, C. Micheletti, L. Di Bari, *Dalton Trans.* **2022**, *51*, 518–523.
[3] F. Zinna, L. Arrico, L. Di Bari, *Chem. Commun.* **2019**, *55*, 6607–6609.
[4] R. Carr, N. H. Evans, D. Parker, *Chem. Soc. Rev.* **2012**, *41*, 7673–7686.
[5] M. Leonzio, A. Melchior, G. Faura, M. Tolazzi, M. Bettinelli, F. Zinna, L. Arrico, L. Di Bari, F. Piccinelli, *New J. Chem.* **2018**, *42*, 7931–7939.
[6] J. Yuasa, T. Ohno, H. Tsumatori, R. Shiba, H. Kamikubo, M. Kataoka, Y. Hasegawa, T. Kawai, *Chem. Commun.* **2013**, *49*, 4604–4606.
[7] S. Yamashita, *IEEE J. Sel. Top. Quantum Electron.* **2001**, *7*, 41–43.
[8] C.-H. Yeh, C.-C. Lee, S. Chi, *IEEE Photonics Technol. Lett.* **2003**, *15*, 1053–1054.
[9] O. G. Willis, F. Petri, G. Pescitelli, A. Pucci, E. Cavalli, A. Mandoli, F. Zinna, L. Di Bari, *Angew. Chem. Int. Ed.* **2022**, *61*, e202208326–e202208326.
[10] N. F. M. Mukthar, N. D. Schley, G. Ung, *J. Am. Chem. Soc.* **2022**, *144*, 6148–6153.
[11] S. W. Magennis, A. J. Ferguson, T. Bryden, T. S. Jones, A. Beeby, I. D. W. Samuel, *Synth. Met.* **2003**, *138*, 463–469.
[12] P. Martín-Ramos, I. R. Martín, F. Lahoz, S. Hernández-Navarro, P. S. Pereira da Silva, I. Hernández, V. Lavín, M. Ramos Silva, *J. Alloys Compd.* **2015**, *619*, 553–559.
[13] Q. Sun, P. Yan, W. Niu, W. Chu, X. Yao, G. An, G. Li, *RSC Adv.* **2015**, *5*, 65856–65861.
[14] M. Deng, N. D. Schley, G. Ung, *Chem. Commun.* **2020**, *56*, 14813–14816.
[15] L. Arrico, C. Benetti, L. Di Bari, *ChemPhotoChem* **2021**, *5*, 815–821.
[16] P. Stachelek, L. MacKenzie, D. Parker, R. Pal, *Nat. Commun.* **2022**, *13*, 553–553.
[17] C. Lincheneau, C. Destribats, D. E. Barry, J. A. Kitchen, R. D. Peacock, T. Gunnlaugsson, *Dalton Trans.* **2011**, *40*, 12056–12059.
[18] D. E. Barry, J. A. Kitchen, L. Mercs, R. D. Peacock, M. Albrecht, T. Gunnlaugsson, *Dalton Trans.* **2019**, *48*, 11317–11325.
[19] M. Starck, L. E. MacKenzie, A. S. Batsanov, D. Parker, R. Pal, *Chem. Commun.* **2019**, *55*, 14115–14118.
[20] A. T. Frawley, R. Pal, D. Parker, *Chem. Commun.* **2016**, *52*, 13349–13352.
[21] J. L. Lunkley, D. Shirotani, K. Yamanari, S. Kaizaki, G. Muller, *J. Am. Chem. Soc.* **2008**, *130*, 13814–13815.
[22] H.-Y. Wong, W.-S. Lo, K.-H. Yim, G.-L. Law, *Chem* **2019**, *5*, 3058–3095.
[23] F. Zinna, L. Di Bari, *Chirality* **2015**, *27*, 1–13.
[24] F. Zinna, U. Giovanella, L. D. Bari, *Adv. Mater.* **2015**, *27*, 1791–1795.
[25] B.-A. N. Willis, D. Schnable, N. D. Schley, G. Ung, *J. Am. Chem. Soc.* **2022**, *144*, 22421–22425.
[26] S. Sato, A. Yoshii, S. Takahashi, S. Furumi, M. Takeuchi, H. Isobe, *Proc. Natl. Acad. Sci.* **2017**, *114*, 13097–13101.
[27] Y. Sang, J. Han, T. Zhao, P. Duan, M. Liu, *Adv. Mater.* **2020**, *32*, 1900110.
[28] E. M. Sánchez-Carnerero, A. R. Agarrabeitia, F. Moreno, B. L. Maroto, G. Muller, M. J. Ortiz, S. de la Moya, *Chem. - Eur. J.* **2015**, *21*, 13488–13500.
[29] C. L. Maupin, R. S. Dickins, L. G. Govenlock, C. E. Mathieu, D. Parker, J. A. G. Williams, J. P. Riehl, *J. Phys. Chem. A* **2000**, *104*, 6709–6717.
[30] R. S. Dickins, J. A. K. Howard, C. L. Maupin, J. M. Moloney, D. Parker, J. P. Riehl, G. Siligardi, J. A. G. Williams, *Chem. – Eur. J.* **1999**, *5*, 1095–1105.
[31] C. L. Maupin, D. Parker, J. A. G. Williams, J. P. Riehl, *J. Am. Chem. Soc.* **1998**, *120*, 10563–10564.

[32] K. Dhbaibi, M. Grasser, H. Douib, V. Dorcet, O. Cador, N. Vanthuyne, F. Riobé, O. Maury, S. Guy, A. Bensalah-Ledoux, B. Baguenard, G. L. J. A. Rikken, C. Train, B. Le Guennic, M. Atzori, F. Pointillart, J. Crassous, *Angew. Chem. Int. Ed.* **2022**, *n/a*, e202215558.

[33] E. Cavalli, C. Nardon, O. G. Willis, F. Zinna, L. Di Bari, S. Mizzoni, S. Ruggieri, S. C. Gaglio, M. Perduca, C. Zaccone, A. Romeo, F. Piccinelli, *Chem. – Eur. J.* **2022**, *28*, e202200574–e202200574.

[34] B. Lefeuvre, C. A. Mattei, J. F. Gonzalez, F. Gendron, V. Dorcet, F. Riobé, C. Lalli, B. Le Guennic, O. Cador, O. Maury, S. Guy, A. Bensalah-Ledoux, B. Baguenard, F. Pointillart, *Chem. – Eur. J.* **2021**, *27*, 7362–7366.

[35] F. Gendron, S. Di Pietro, L. Abad Galán, F. Riobé, V. Placide, L. Guy, F. Zinna, L. Di Bari, A. Bensalah-Ledoux, Y. Guyot, G. Pilet, F. Pointillart, B. Baguenard, S. Guy, O. Cador, O. Maury, B. Le Guennic, *Inorg. Chem. Front.* **2021**, *8*, 914–926.

[36] J. R. Jiménez, S. Míguez-Lago, M. Poncet, Y. Ye, C. Lopez, C. M. Cruz, A. G. Campaña, E. Colacio, C. Piguet, J. M. Herrera, *J. Mater. Chem. C* **2023**.

[37] Y. Cheng, J. He, W. Zou, X. Chang, Q. Yang, W. Lu, *Chem. Commun.* **2023**.

[38] J.-R. Jiménez, M. Poncet, S. Míguez-Lago, S. Grass, J. Lacour, C. Besnard, J. M. Cuerva, A. G. Campaña, C. Piguet, *Angew. Chem. Int. Ed.* **2021**, *60*, 10095–10102.

[39] J.-R. Jiménez, B. Doistau, C. M. Cruz, C. Besnard, J. M. Cuerva, A. G. Campaña, C. Piguet, *J. Am. Chem. Soc.* **2019**, *141*, 13244–13252.

[40] C. Dee, F. Zinna, W. R. Kitzmann, G. Pescitelli, K. Heinze, L. Di Bari, M. Seitz, *Chem. Commun.* **2019**, *55*, 13078–13081.

[41] M. Cantuel, G. Bernardinelli, G. Muller, J. P. Riehl, C. Piguet, *Inorg. Chem.* **2004**, *43*, 1840–1849.

[42] J. P. Riehl, F. S. Richardson, *Chem. Rev.* **1986**, *86*, 1–16.

[43] L. Arrico, L. Di Bari, F. Zinna, *Chem. – Eur. J.* **2021**, *27*, 2920–2934.

[44] S. F. Mason, S. F. Mason, *Molecular Optical Activity and the Chiral Discriminations*, Cambridge University Press, **1982**.

[45] F. S. Richardson, *Inorg. Chem.* **1980**, *19*, 2806–2812.

[46] W. R. Kitzmann, J. Moll, K. Heinze, *Photochem. Photobiol. Sci.* **2022**, *21*, 1309–1331.

[47] W. R. Kitzmann, K. Heinze, *Angew. Chem. Int. Ed.* **2023**.

[48] S. Otto, M. Dorn, C. Förster, M. Bauer, M. Seitz, K. Heinze, *Coord. Chem. Rev.* **2018**, *359*, 102–111.

[49] F. Reichenauer, C. Wang, C. Förster, P. Boden, N. Ugur, R. Báez-Cruz, J. Kalmbach, L. M. Carrella, E. Rentschler, C. Ramanan, G. Niedner-Schatteburg, M. Gerhards, M. Seitz, U. Resch-Genger, K. Heinze, *J. Am. Chem. Soc.* **2021**, *143*, 11843–11855.

[50] J. Kalmbach, C. Wang, Y. You, C. Förster, H. Schubert, K. Heinze, U. Resch-Genger, M. Seitz, *Angew. Chem. Int. Ed.* **2020**, *59*, 18804–18808.

[51] S. Otto, C. Förster, C. Wang, U. Resch-Genger, K. Heinze, *Chem. - Eur. J.* **2018**, *24*, 12555–12563.

[52] S. Treiling, C. Wang, C. Förster, F. Reichenauer, J. Kalmbach, P. Boden, J. P. Harris, L. M. Carrella, E. Rentschler, U. Resch-Genger, C. Reber, M. Seitz, M. Gerhards, K. Heinze, *Angew. Chem. Int. Ed.* **2019**, *58*, 18075–18085.

[53] C. Wang, S. Otto, M. Dorn, E. Kreidt, J. Lebon, L. Sršan, P. Di Martino-Fumo, M. Gerhards, U. Resch-Genger, M. Seitz, K. Heinze, *Angew. Chem. Int. Ed.* **2018**, *57*, 1112–1116.

[54] S. Otto, M. Grabolle, C. Förster, C. Kreitner, U. Resch-Genger, K. Heinze, *Angew. Chem. Int. Ed.* **2015**, *54*, 11572–11576.

[55] O. S. Wenger, *J. Am. Chem. Soc.* **2018**, *140*, 13522–13533.

[56] C. Wegeberg, O. S. Wenger, *JACS Au* **2021**, *1*, 1860–1876.

[57] C. Li, P. Duan, *Chem. Lett.* **2021**, *50*, 546–552.

[58] L. E. MacKenzie, L.-O. Pålsson, D. Parker, A. Beeby, R. Pal, *Nat. Commun.* **2020**, *11*, 1676.

[59] B. Baguenard, A. Bensalah-Ledoux, L. Guy, F. Riobé, O. Maury, S. Guy, *Nat. Commun.* **2023**, *14*, 1065.

[60] E. Huskowska, C. Maupin, D. Parker, J. G. Williams, J. Riehl, *Enantiomer* **1997**, *2*, 381–395.

[61] S. Aime, A. S. Batsanov, M. Botta, J. A. Howard, D. Parker, K. Senanayake, G. Williams, *Inorg. Chem.* **1994**, *33*, 4696–4706.

[62] Z. Ahmed, R. E. Aderne, J. Kai, J. A. Resende, M. Cremona, *Polyhedron* **2016**, *117*, 518–525.

[63] S. Meshkova, Z. Topilova, D. Bolshoy, S. Beltyukova, M. Tsvirko, V. Y. Venchikov, *Acta Phys. Pol. A* **1999**, *95*, 983–990.

[64] F. Zinna, T. Bruhn, C. A. Guido, J. Ahrens, M. Bröring, L. Di Bari, G. Pescitelli, *Chem. Eur. J.* **2016**, *22*, 16089–16098.

[65] F. Gendron, B. Moore II, O. Cador, F. Pointillart, J. Autschbach, B. Le Guennic, *J. Chem. Theory Comput.* **2019**, *15*, 4140–4155.

[66] R. Berardozzi, L. Di Bari, *ChemPhysChem* **2015**, *16*, 2868–2875.

[67] R. Berardozzi, G. Pescitelli, S. Di Pietro, C. Resta, F. P. Ballistreri, A. Pappalardo, G. A. Tomaselli, L. Di Bari, *Chirality* **2015**, *27*, 857–863.

[68] A. Abhervé, M. Mastropasqua Talamo, N. Vanthuyne, F. Zinna, L. Di Bari, M. Grasser, B. Le Guennic, N. Avarvari, *Eur. J. Inorg. Chem.* **2022**, *2022*.

[69] F. Gendron, M. Grasser, B. Le Guennic, *Phys. Chem. Chem. Phys.* **2022**, *24*, 5404–5410.

[70] J. P. Leonard, P. Jensen, T. McCabe, J. E. O'Brien, R. D. Peacock, P. E. Kruger, T. Gunnlaugsson, *J. Am. Chem. Soc.* **2007**, *129*, 10986–10987.

[71] K. T. Hua, J. Xu, E. E. Quiroz, S. Lopez, A. J. Ingram, V. A. Johnson, A. R. Tisch, A. de Bettencourt-Dias, D. A. Straus, G. Muller, *Inorg. Chem.* **2012**, *51*, 647–660.

[72] H. Sasai, T. Suzuki, S. Arai, T. Arai, M. Shibasaki, *J. Am. Chem. Soc.* **1992**, *114*, 4418–4420.

[73] J. R. Robinson, X. Fan, J. Yadav, P. J. Carroll, A. J. Wooten, M. A. Pericàs, E. J. Schelter, P. J. Walsh, *J. Am. Chem. Soc.* **2014**, *136*, 8034–8041.

[74] J. D. van der Laan, J. B. Wright, S. A. Kemme, D. A. Scrymgeour, *Appl. Opt.* **2018**, *57*, 5464.

[75] O. G. Willis, A. Pucci, E. Cavalli, F. Zinna, L. Di Bari, *J. Mater. Chem. C* **2023**, 10.1039.D3TC00034F.

[76] J.-C. G. Bünzli, S. V. Eliseeva, in *Lanthan. Lumin. Photophysical Anal. Biol. Asp.* (Eds.: P. Hänninen, H. Härmä), Springer Berlin Heidelberg, Berlin, Heidelberg, **2011**, pp. 1–45.

[77] C. A. Emeis, L. J. Oosterhoff, *Chem. Phys. Lett.* **1967**, *1*, 129–132.

10.1002/anie.202302358

WILEY-VCH

MINIREVIEW

Entry for the Table of Contents

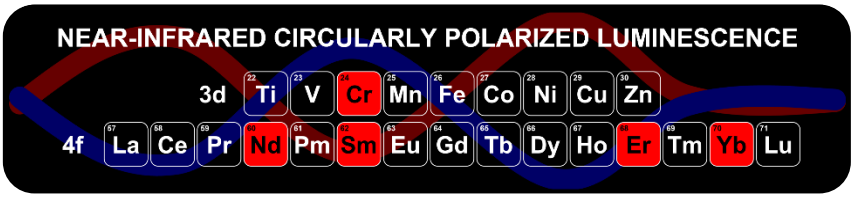

This mini-review aims to catalogue all accounts of lanthanide and d-metal chiral complexes which show circularly polarized luminescence (CPL) in the near-infrared (NIR). Recent improvements in the rational design of suitable complexes which show strong emission properties and high chiroptical activity will be discussed, as well as the setups capable of measuring NIR-CPL.

Institute and/or researcher Twitter usernames: @ChemUniPi, @DscmPisa, @Hel4chiroled, @Olliewillis0805, @LorenzoDiBari6